



HAL
open science

Mass transfer development over large rectangular wall region governed by secondary flows

Florian Huchet, David Kramolis, Jaromir Havlica

► To cite this version:

Florian Huchet, David Kramolis, Jaromir Havlica. Mass transfer development over large rectangular wall region governed by secondary flows. Congrès de la Société Française de Génie des Procédés, Oct 2019, Nantes, France. <hal-04343594>

HAL Id: hal-04343594

<https://hal.science/hal-04343594v1>

Submitted on 10 Sep 2024

HAL is a multi-disciplinary open access archive for the deposit and dissemination of scientific research documents, whether they are published or not. The documents may come from teaching and research institutions in France or abroad, or from public or private research centers.

L'archive ouverte pluridisciplinaire HAL, est destinée au dépôt et à la diffusion de documents scientifiques de niveau recherche, publiés ou non, émanant des établissements d'enseignement et de recherche français ou étrangers, des laboratoires publics ou privés.



Distributed under a Creative Commons CC BY-NC 4.0 - Attribution - Non-commercial use - International License

Mass transfer development over large rectangular wall region governed by secondary flows



Florian Huchet¹, David Kramolis², Jaromir Havlica^{2,3}

1 – IFSTTAR-UGE, Allée des Ponts et Chaussées, CS 5004, 44344, Bouguenais cedex, France

2 - Jan Evangelista Purkyně University in Ústí nad labem, Ceske mladeze 8, 400 96 Usti nad Labem, Czech Republic

3 - Czech Academy of Sciences, Institute of Chemical Process Fundamentals, Rozvojova 2/135, 165 02 Prague, Czech Republic

Mass transfer probes: measurement of wall shear stress

- Advantages:
 - can be used in a wide variety of flow;
 - no interference with the flow;
 - possibility of measuring time-varying flows;
 - in the case of electro-chemical probes: calibration is not necessary.
- Two basic spatial orientations between probe main edge and fluid flow:
 - perpendicular transfer surface, see Fig. 1b);
 - slanted transfer surface, see Fig. 1c).
- Governing equation of mass transport:

$$\frac{\partial c}{\partial t} + u_x \frac{\partial c}{\partial x} + u_y \frac{\partial c}{\partial y} + u_z \frac{\partial c}{\partial z} = D \frac{\partial^2 c}{\partial x^2} + D \frac{\partial^2 c}{\partial y^2} + D \frac{\partial^2 c}{\partial z^2} \quad (1)$$

- boundary conditions:

$$\begin{aligned} x \rightarrow -\infty \quad z > 0 \quad c &= c_\infty \\ x \in (0, L_x) \quad z = 0 \quad c &= c_w \\ x < 0 \cup x > L_x \quad z = 0 \quad \frac{\partial c}{\partial z} &= 0 \\ \forall x \quad z \rightarrow \infty \quad c &= c_\infty \end{aligned} \quad (2)$$

- Assumptions:

- steady or pseudo-steady state $\rightarrow \frac{\partial c}{\partial t} = 0$;
- the flow is homogeneous over the surface of the probe;
- convection is large enough that diffusion in the x direction can be neglected $\rightarrow D \frac{\partial^2 c}{\partial x^2} \approx 0$;
- concentration is changed negligibly in direction $y \rightarrow D \frac{\partial^2 c}{\partial y^2} \approx 0$;
- diffusion boundary layer thickness, δ_D , is smaller than the thickness of hydrodynamical boundary layer, $\delta_H \rightarrow u_x = S_x z$; $u_y = S_y z$, see Fig. 1a);
- a) for perpendicular transfer surface: $u_x \gg u_y, u_z \rightarrow u_y, u_z \approx 0$;
b) for slanted transfer surface: $u_x, u_y \gg u_z \rightarrow u_z \approx 0$.

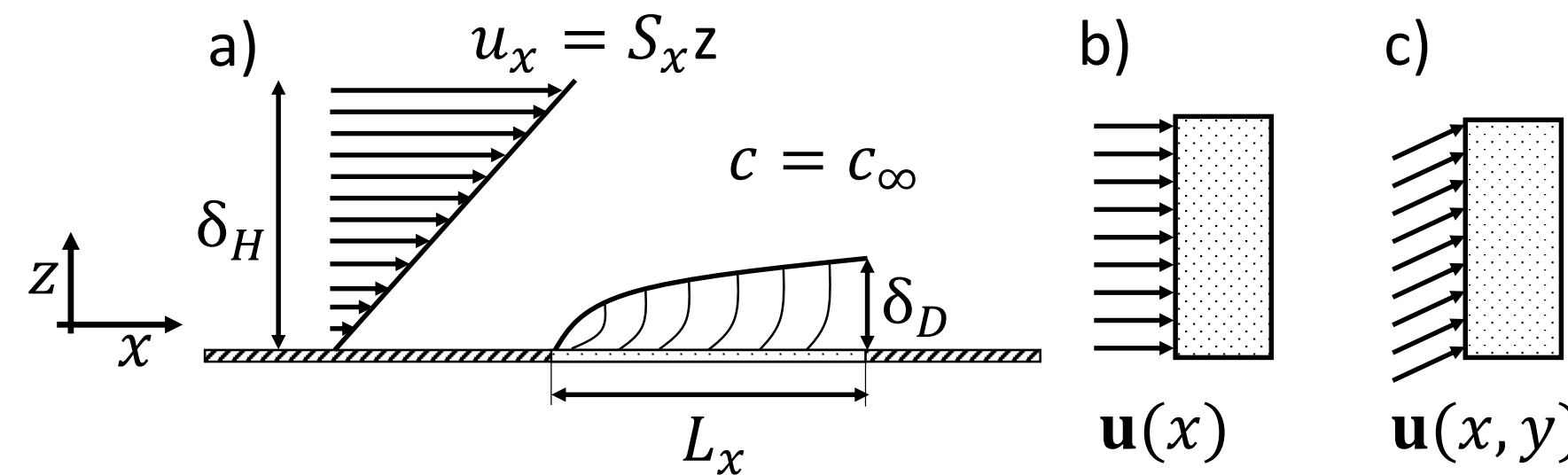


Figure 1: a) Description of mass transfer in the close of the probe; b) perpendicular transfer surface; c) slanted transfer surface.

Perpendicular transfer surface

- Simplification of eq. (1) according to the assumptions (1 - 6):

$$S_x z \frac{\partial c}{\partial x} = D \frac{\partial^2 c}{\partial z^2}; \quad (3)$$

- Analytical solution of eq. (3):

$$\frac{c - c_w}{c_\infty - c_w} = \frac{1}{\Gamma(4/3)} \int_0^\eta e^{-\eta^2} d\eta; \quad \eta = \frac{z}{L_x^{1/3}} \left[\frac{S_x}{9D} \right]^{1/3} \quad (4)$$

- Evaluation of mass transfer coefficient (Léveque solution) on the base of eqs. (3) and (4):

$$\bar{k}_z = \frac{3}{2\Gamma(4/3)9^{1/3}} \left(\frac{D^2 S_x}{L_x} \right)^{1/3} = 0.8075 \left(\frac{D^2 S_x}{L_x} \right)^{1/3} \quad (5)$$

- Normalized Sherwood number:

$$\text{Sh}^* = \frac{\text{Sh}}{\text{Pe}_s^{1/3}} = \frac{\bar{k}_z L_x}{D} = \bar{k}_z \left(\frac{L_x}{D^2 S_x} \right)^{1/3} = 0.8075 \quad (6)$$

Slanted transfer surface

- Simplification of eq.(1) according to the assumptions (1 - 6):

$$S_x z \frac{\partial c}{\partial x} + S_y z \frac{\partial c}{\partial y} = D \frac{\partial^2 c}{\partial z^2} \quad (7)$$

- No analytical solution of eq. (7), but it is possible to find out:

- analytical solution of l_{eq} and Sh^* ;
- numerical solution of concentration profiles and Sh^* .

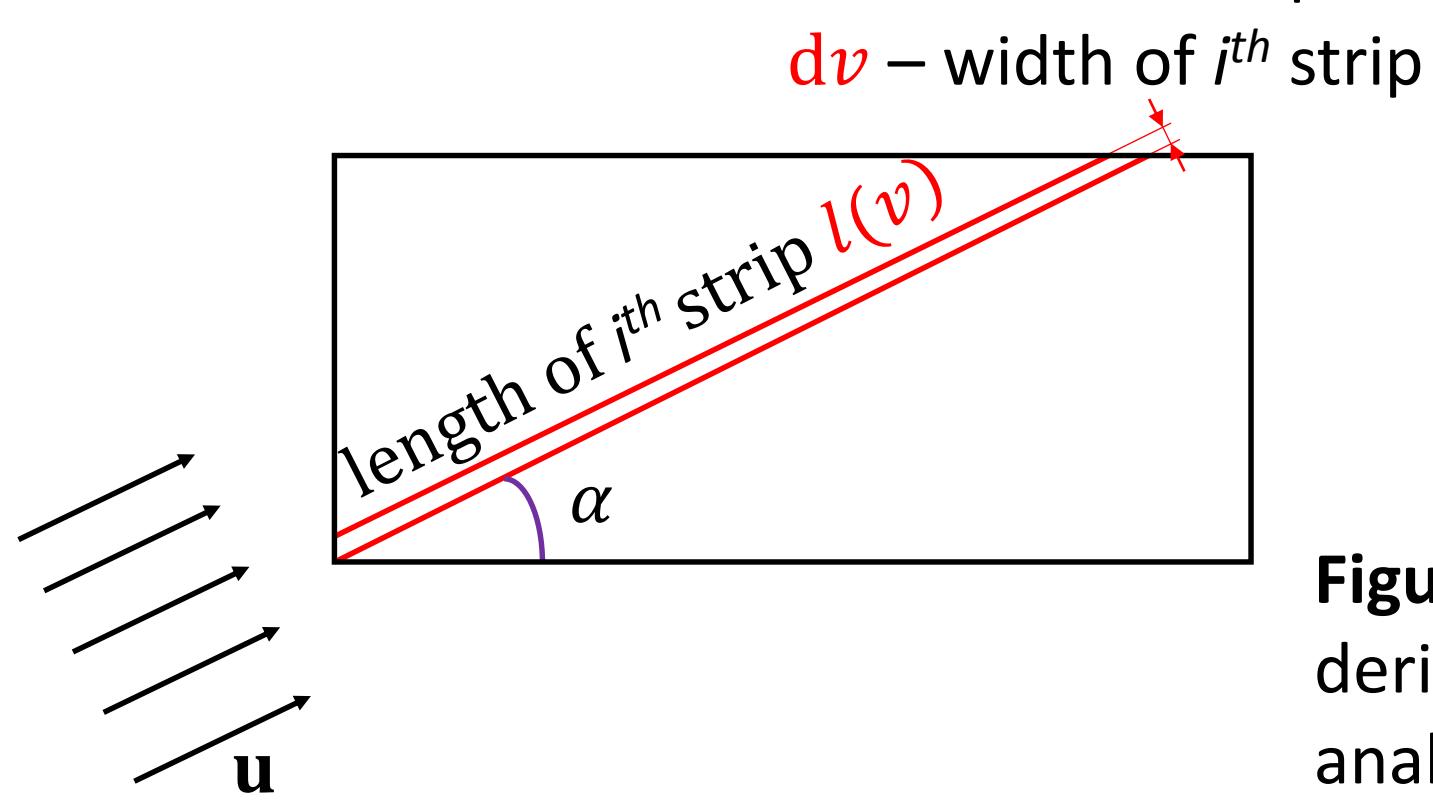


Figure 2: Scheme for derivation of analytical l_{eq} and Sh^*

Analytical solution of equivalent length and normalized Sherwood number

- Mass transfer coefficient for i^{th} strip is defined as:

$$k_z = 0.8075 \left(\frac{D^2 \|S\|}{l(v)} \right)^{1/3} \quad (8)$$

- The mass transfer coefficient for the whole probe is evaluation on the base of summation (integral) of all stripes over the entire surface of the probe. :

$$\bar{k}_z = \frac{1}{L_x L_y} \int k_z l(v) dv = 0.8075 \frac{(D^2 \|S\|)^{1/3}}{L_x L_y} \int l(v)^{2/3} dv = 0.8075 \left(\frac{D^2 \|S\|}{l_{eq}} \right)^{1/3} \quad (9)$$

- Evaluation of equivalent length l_{eq} :

$$l_{eq}^{1/3} = \frac{L_x L_y}{\int_v l(v)^{2/3} dv} = \begin{cases} \frac{L_x^{1/3}}{(1-\beta)^{1/6} \left(1 + \frac{R\sqrt{\beta}}{5\sqrt{1-\beta}} \right)} & \text{for } \beta \leq \beta_c \\ \frac{L_x^{1/3}}{\beta^{1/6} R^{1/3} \left(1 + \frac{\sqrt{1-\beta}}{5R\sqrt{\beta}} \right)} & \text{for } \beta > \beta_c \end{cases} \quad \text{where } \beta_c = \frac{1}{1+R^2} \quad (10)$$

- The normalize Sherwood number Sh^* is defined as:

$$\text{Sh}^* = \frac{\text{Sh}}{\text{Pe}_s^{1/3}} = \bar{k}_z \left(\frac{l}{D^2 \|S\|} \right)^{1/3} = 0.8075 \left(\frac{D^2 \|S\|}{l_{eq}} \right)^{1/3} \left(\frac{l}{D^2 \|S\|} \right)^{1/3} = 0.8075 \left(\frac{l}{l_{eq}} \right)^{1/3} \quad (11)$$

- The resulting value of the Sh^* is dependent on the choice of length l in the eq. (11), see Fig. 3:

$$\text{Sh}^* = \begin{cases} 0.8075 (1-\beta)^{1/6} \left(1 + \frac{R\sqrt{\beta}}{5\sqrt{1-\beta}} \right) & \text{for } l = L_x; \beta \leq \beta_c \\ 0.8075 \beta^{1/6} R^{1/3} \left(1 + \frac{\sqrt{1-\beta}}{5R\sqrt{\beta}} \right) & \text{for } l = L_x; \beta > \beta_c \\ 0.8075 & \text{for } l = l_{eq}; \forall \beta \end{cases} \quad (12)$$

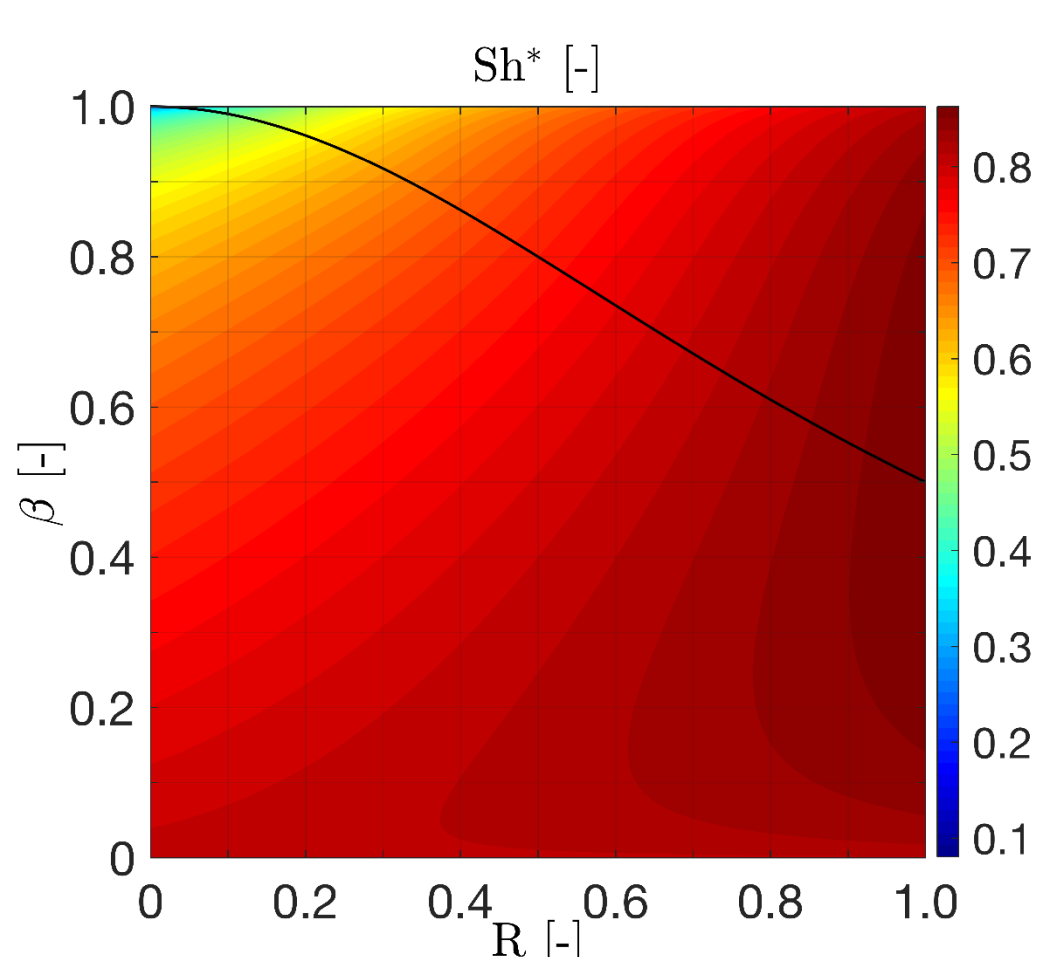


Figure 3: Normalized Sherwood number evaluated for length $l = L_x$ in dependence on the parameters β and ratio R . Black curve describes the value of critical β_c .

Numerical solution of concentrations profile and normalized Sherwood number

- Definition of hydrodynamical parameter β and non-dimensional characteristics of the system:

$$\beta = \frac{S_y^2}{S_x^2 + S_y^2} = \frac{S_y^2}{\|S\|^2} \Rightarrow S_x = \sqrt{1-\beta} \|S\|; S_y = \sqrt{\beta} \|S\| \quad (13)$$

$$c^+ = \frac{c - c_w}{c_\infty - c_w}; x^+ = \frac{x}{L_x}; y^+ = \frac{y}{L_y}; z^+ = \frac{z}{\delta_D}; \delta_D = \left(\frac{Dl}{\|S\|} \right)^{1/3}; R = \frac{L_x}{L_y} \quad (14)$$

- Modification of eq. (7):

$$\frac{\partial c^+}{\partial x^+} + \frac{\sqrt{\beta} R}{\sqrt{1-\beta}} \frac{\partial c^+}{\partial y^+} = \frac{1}{z^+ \sqrt{1-\beta}} \frac{\partial^2 c^+}{(\partial z^+)^2} \quad (15)$$

- Numerical solution of eq. (7), see Fig. 4. The shape of the concentration profiles is dependent on the parameters β and ratio R .

- Sh^* is evaluated from derivative of concentration in the z direction on the probe surface using a relation, see Fig. 5:

$$\text{Sh}^* = \int_0^1 \int_0^1 - \frac{\partial c^+}{\partial z^+} dx^+ dy^+ \quad (16)$$

- Final values of Sh^* is dependent on the choice of length l . For example, the length l can be replaced by the width of the electrode L_x or by the equivalent length:

- $l = L_x$ and for $\forall \beta$:

$$\frac{\partial c^+}{\partial x^+} + \frac{\sqrt{\beta} R}{\sqrt{1-\beta}} \frac{\partial c^+}{\partial y^+} = \frac{1}{z^+ \sqrt{1-\beta}} \frac{\partial^2 c^+}{(\partial z^+)^2} \Rightarrow \text{Sh}^*(R, \beta), \text{ see Fig. 3} \quad (17)$$

- $l = l_{eq}$ and for $\beta \leq \beta_c$:

$$\frac{\partial c^+}{\partial x^+} + \frac{\sqrt{\beta} R}{\sqrt{1-\beta}} \frac{\partial c^+}{\partial y^+} = \frac{1}{z^+ \sqrt{1-\beta}} \sqrt{1-\beta} \left(1 + \frac{R\sqrt{\beta}}{5\sqrt{1-\beta}} \right)^3 \frac{\partial^2 c^+}{(\partial z^+)^2} \Rightarrow \text{Sh}^* = 0.8075 \quad (18)$$

- $l = l_{eq}$ and for $\beta > \beta_c$:

$$\frac{\partial c^+}{\partial x^+} + \frac{\sqrt{\beta} R}{\sqrt{1-\beta}} \frac{\partial c^+}{\partial y^+} = \frac{1}{z^+ \sqrt{1-\beta}} \sqrt{\beta} R \left(1 + \frac{\sqrt{1-\beta}}{5R\sqrt{\beta}} \right)^3 \frac{\partial^2 c^+}{(\partial z^+)^2} \Rightarrow \text{Sh}^* = 0.8075 \quad (19)$$

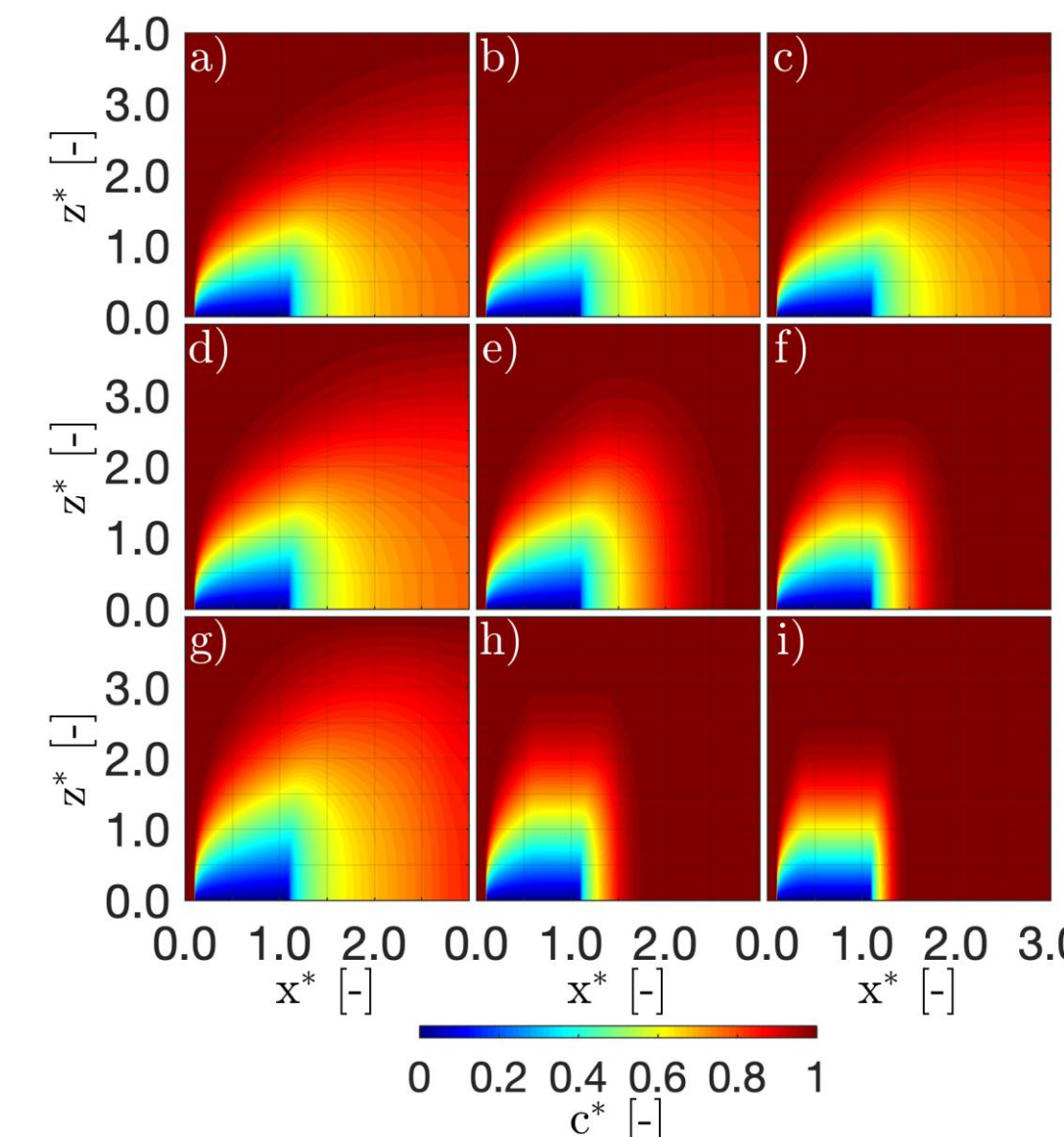


Figure 4: Concentration profile in the plane x^+z^+ for $y^+ = L_y/2$: 1st row - $\beta = 0$; 2nd row - $\beta = 0.4$; 3rd row - $\beta = 0.8$; 1st column - $R = 0.1$; 2nd column - $R = 0.4$; 3rd column - $R = 0.8$.

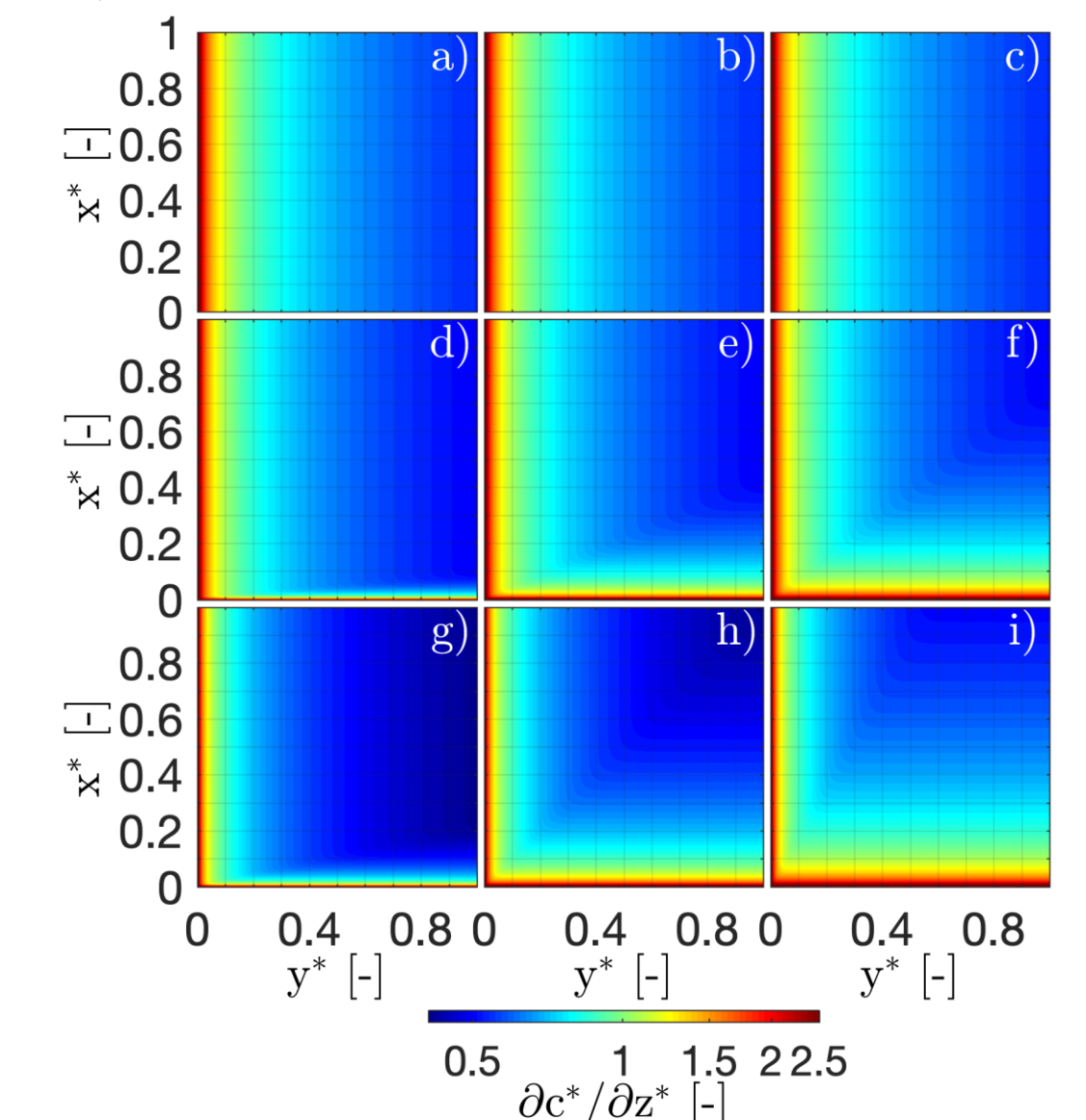


Figure 5: Derivative of concentration in the z direction on the probe surface (logarithmic colorbar): 1st row - $\beta = 0$; 2nd row - $\beta = 0.4$; 3rd row - $\beta = 0.8$; 1st column - $R = 0.1$; 2nd column - $R = 0.4$; 3rd column - $R = 0.8$.

Conclusion:

We have derived an equation describing the equivalent length and normalized Sherwood number as a function of the fluid flow angle (characterized by parameter β) and the aspect ratio of the rectangular mass transfer probe ($R = L_x/L_y$). The given equations could serve for better interpretation of the measurement of wall shear stress (ED or hot-film method) especially for fluid flow associated with secondary flows.

Acknowledgment:

This research was supported by the grant UJEP-SGS-2018-53-002-2.